Check for updates

Selectively mixed matrix hemodialysis membrane for adequate clearance of *p*-cresol by the incorporation of imprinted zeolite

Yanuardi Raharjo, [ID] *[a] Ahmad Fauzi Ismail,[b] Mohd Hafiz Dzarfan Othman, [ID] [b] Mochamad Zakki Fahmi, [ID] [a] Saiful, [ID] [c] Djoko Santoso,[d] Mochamad Ifan Nugroho,[a] Diana Merna,[a] Maipha Deapati Arief[a] and Risma Chikita Pratama[a]

The adequacy in uremic toxin removal upon hemodialysis treatment is essential in patients with kidney failure diseases as poor removal leads to heart failure, hypertension, and stroke. The combination of adsorption and diffusion processes has become very advantageous for hemodialysis membranes. By this mechanism, water-soluble uremic toxins (WSUTs) and protein-bounded uremic toxins (PBUTs) could be removed at one time. Therefore, this study aimed to develop a novel imprinted zeolite by *p*-cresol (IZC) and then incorporated it into polyethersulfone (PES) and poly(vinyl pyrrolidone) (PVP) to produce hollow fiber mixed matrix membrane (HF-MMM). The IZC proved to be sensitive in attracting the adsorbate, classifying it as having a strong adsorption behavior. Accordingly, IZC is very promising to be applied as an adsorbent in the hemodialysis treatment. In this study, IZC as *p*-cresol's adsorbent was incorporated into a PES-based polymeric membrane with a small addition of PVP to produce HF-MMM using a dry/wet spinning process. The effect of air gap distance between the spinneret and coagulant bath and percentage loading for PES, PVP, and IZC were studied and optimized to obtain the best performance of HF-MMM. The 40 cm of air gap distance, 16 wt% of PES, 2 wt% of PVP, and 1 wt% of IZC loading were able to produce a superior hemodialysis membrane. These optimized parameters showed sufficient uremic toxin removal, *i.e.*, 60.74% of urea, 52.35% of *p*-cresol in the phosphate buffer saline solution, and 66.29% of *p*-cresol in bovine serum albumin solution for 4 h permeation using the dialysis system. These HF-MMMs also achieved pure water flux of 67.57 L m^{-2} h^{-1} bar^{-1} and bovine serum albumin rejection of 95.05%. Therefore, this membrane has proven to be able to clean up WSUT and PBUT through a one-step process. Moreover, as compared to the neat PES membrane, MMM was able to remove *p*-cresol at 186.22 times higher capability.

Introduction

Membrane technology is widely applied to support the development of science and technology, both in terms of theoretical physics and chemistry. The application starts from secondary human needs such as water filters[1] and gas separation[2] to primary human needs, such as an artificial kidney.[3] Regarding its application, membrane technology is used to treat kidney disease *via* hemodialysis (HD) treatment. Various membranes have been developed by researchers for HD treatment. There are

two types of membranes that are commercially available and widely used in hospitals and dialysis clinics to treat patients with kidney failure. The first one is the low-flux dialysis membrane, in which the membrane can remove much of the water-soluble uremic toxins (WSUTs), such as urea, creatinine, and uric acid. However, it is difficult to remove the middle molecular-weight water-soluble uremic toxins (MWUT), such as cystatin C, β$_2$-microglobulin, and β-endorphin, as well as protein-bounded uremic toxins (PBUTs), such as indoxyl sulfate, *p*-cresol, and phenol.[4] Moreover, the MWUT and PBUT are dangerous if they accumulate in the blood, as they may cause endothelial or leukocyte dysfunction and exert proinflammatory and hepatotoxic effects that contribute to increased mortality.[5] The second type of HD membrane is a high-flux dialysis membrane. This membrane can remove some uremic toxins, which cannot be eliminated by a low-flux dialysis membrane.[6] This membrane uses a higher pressure under larger pores compared to a low-flux dialysis membrane. Through this, the removal of MWUT and PBUT is forced *via*

[a]*Membrane Science and Technology Research Group (MSTRG), Chemistry Department, Faculty of Science and Technology, Universitas Airlangga, Surabaya 60115, Indonesia. E-mail: yanuardiraharjo@fst.unair.ac.id*

[b]*Advanced Membrane Technology Research Centre (AMTEC), Universiti Teknologi Malaysia, Skudai 81310, Malaysia*

[c]*Chemistry Department, Faculty of Mathematics and Natural Science, Universitas Syiah Kuala, Banda Aceh, Indonesia*

[d]*Division of Nephrology and Hypertension, Dr Soetomo Hospital, Faculty of Medicine, Universitas Airlangga, Surabaya 60115, Indonesia*

high pressure and large pore size.[7] Regarding HD, the adequacy of dialysis fulfilled by high-flux dialysis compared to low-flux dialysis has been reported.[8]

Besides, the high-flux membrane, another treatment that can be applied to remove MWUT and PBUT in blood purification is by using an adsorption mechanism called hemoperfusion (HP). Basically, the mechanism of HP involves the hydrophobic properties of the sorbents or chemical affinity.[9] Carbon-based adsorbents, such as activated carbon (AC), have been used internally by oral or in extracorporeal devices.[10] An HP column is a simple device, in which a plastic column is filled with the adsorbent powder. The uncoated and coated charcoal were evaluated as adsorbents to eliminate the MWUT and PBUT. When the uncoated charcoal is used, the MWUT and PBUT can clearly be adsorbed better by the adsorbents compared with the coated charcoal. Nonetheless, the main problem is biocompatibility. The uncoated charcoal is highly incompatible with blood through direct contact, as it adsorbs not only the MWUT and PBUT but also other proteins that are still needed by the body due to the hydrophobic properties of the sorbent. Based on the previous works, they stated that one hour of HP treatment was as effective as four hours using HD treatment.[7,11] In the past, HP is rarely used for blood purification applications primarily due to the biocompatibility issue of materials, particle release, and limitation to removing the WSUT despite having a very strong capability to remove MWUT and PBUT. With advanced manufacturing processes and improved biocompatibility, sorbent has enormous potential to be developed.[12] Hence, the type of materials applied for HP application needs to be improved and innovated. The high selectivity of hydrophilic sorbents might also be very effective and beneficial for eliminating the MWUT and PBUT.

A combination of the strengths of HD and HP can be very beneficial for blood purification. The module is a polymer membrane used to combine the diffusion and adsorption mechanism at one step called mixed-matrix membrane (MMM).[13] MMM exhibits many advantages, such as flexible large-scale operation, simplicity, time efficiency, minimum membrane fouling, flux decline, and energy saving.[14] The principle of MMM involves synergism of different functions by different materials.[15] The purpose of developing this membrane is to harness its time efficiency during HD application since it is able to remove WSUT, MWUT, and PBUT in one-step dialysis. Besides that, MMM is also able to improve the biocompatibility of a polymer. Apart from that, there can also be a combination of main polymer and inorganic materials, such as multi-walled carbon nanotubes;[16] activated carbon;[17] nano-hydroxyapatite;[18] and silicalite or zeolite.[19] However, there are requirements that need to be fulfilled for a material to be used as an additive, such as that containing a hydrophilic group and being biocompatible and non-toxic. When the main polymer, such as polyethersulfone (PES), is in direct contact with blood during the HD process, the proteins tend to be adsorbed onto the polymer surface. Then, this protein layer causes fouling on the inner surface of the HD membrane and decreases the function of pores in the inner membrane surface.[20] This membrane is a problem-solving for many cases and weaknesses occur during

blood purification treatment. Therefore, there is a need to further study the MMM to provide the best solution for blood purification.

The porous structure of zeolites makes them true shape-selectivity molecular sieves with wide-ranging applications in catalysis, ion exchange, and adsorption processes.[21,22] Other than that, zeolites can be modified through their selectivity of the pore size by the molecularly imprinting polymer (MIP) concept. Khasanah *et al.* (2013)[23] managed to produce an imprinted zeolite for the improvement of the selectivity of a voltammetry sensor in uric acid analysis. This imprinted zeolite-modified glass carbon showed good performance and high sensitivity, precision, accuracy, and low detection limit. Zeolite can be synthesized with a three-dimensionally ordered mesoporous-imprinted structure using a carbon template to improve the catalytic and separation performance.[24] Furthermore, previously, research imprinted zeolite-Y has been developed for *p*-cresol removal applied to hemodialysis.[25]

In this research, PES membranes were produced by combining the imprinted zeolite by *p*-cresol (IZC) with a mixed matrix membrane (MMM). Membranes were produced in a hollow fiber form through a dry-wet jet spinning method using a single-layer spinneret. Thus, the parameters investigated to obtain the best morphologies and performance for urea and *p*-cresol removal water flux, bovine serum albumin (BSA) rejection, and hydrophilicity were air gap distance between the spinneret and coagulant bath and percentage loading of PES. This study aimed to produce the low flux superior membrane to efficiently remove WSUT, MWUT, and PBUT during the treatment in order to provide a better quality of life for patients with kidney failure at one time.

Experimental

Materials

The fabrication of hollow fiber-mixed matrix membrane (HF-MMM) involved PES (Veradel A-301) that was obtained from Solvay Advanced Polymer (USA), PVP K90 (360.000 g mol^{-1}) was obtained from Sigma-Aldrich (USA), NMP 99.5% (MW = 99.1 g mol^{-1}) as a solvent was obtained from Acros Organic, IZC as a sorbent to become a novel selective HF-MMM specific to *p*-cresol as target uremic toxins was obtained from the previous experiment.[22] The *p*-cresol as a target PBUT and urea as a representative of WSUT were obtained from Sigma-Aldrich (USA).

Procedure

Preparation of dope solution. For the fabrication of MMM, PES was used as the main polymer, PVP as an additional polymer to increase the hydrophilicity and pore-forming agent, NMP as a solvent, and IZC as the adsorbent or additive/filler. The IZC loading and PVP loading used in this study were 1 and 1.4 wt%, respectively. The pellet of the PES was dried in an oven at 50 °C for 24 h before use to eliminate the moisture content. Firstly, the dispersant, PES was dissolved in NMP under vigorous stirring. Once a homogenous solution was

Table 1 Dope composition for HF-MMM studied

Variation	PES (wt%)	PVP (wt%)	NMP (wt%)	IZC (wt%)
P14	14	1.4	83.6	1
P16	16	1.4	81.6	1
P18	18	1.4	79.6	1

formed, the pre-dried zeolite powder was slowly added into the PES solution and was followed by the addition of the remaining NMP and PVP. While the materials of the dope solution were in the bottle, a heating step of 60 °C for 2 h was added to help the dissolution process. Then, stirring was continued for 1 day under these conditions to maximize dissolution and remove the trapped air contained in the dope. It can disturb the formation of the uniform HF precursor by producing a deformation in the structure. Besides studying the variation of the IZC loading, PES and PVP loading were also investigated in this study. The PES loading was varied from 14, 16, and 18%. The composition of the dope solution is illustrated in Table 1. The dope solution viscosity was measured using a Cole-Parmer® viscometer (model EW-98965-40, USA).

Hollow fiber membranes fabrication. Hollow fiber membranes were fabricated using an orifice single-layer spinneret with 0.4/0.8 mm as a size for inner and outer diameters (Fig. 1) and a dry/wet spinning machine, as shown in Fig. 2. The spinneret was placed hanging above the tap water surface in the coagulant bath with a distance varying from 10, 20, 30, 40, and 50 cm to study the best performance. The setting for the spinning machine condition was dope extrusion rate was 1 mL min^{-1}, bore fluid pumping speed was 1 mL min^{-1}, bore fluid composition was distilled water, collection speed was 10 m min^{-1}, and bath temperature was 25 °C. After obtaining the hollow fiber membrane, it was washed for 48 h using tap water to remove the solvent, then immersed in 10 wt% glycerol for 24 h in order to improve the membrane wettability and pore collapse.
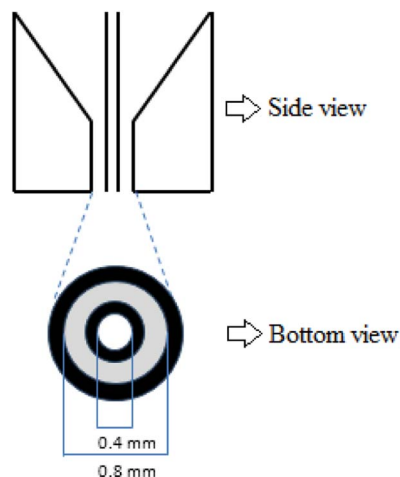

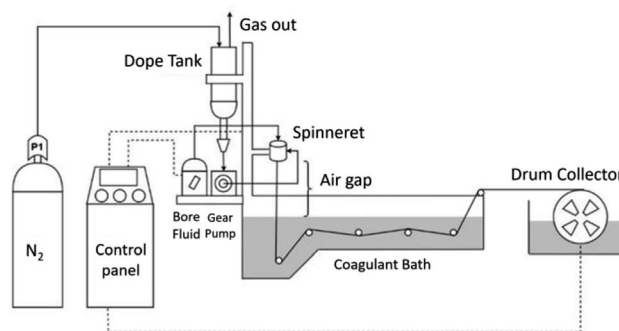**Fig. 1** Spinneret of HF-MMM on the side- and bottom-view.

Fig. 2 Schematic diagram of HF spinning.

Hollow fiber membrane characterization

Scanning electron microscopy (SEM). The structural morphology of the HF-MMM produced was observed using a field-emission scanning electron microscope (TM3000, Hitachi, USA). The inner surface, outer surface, and cross-section views were observed.

Water contact angle (WCA). The contact angle of the surface membranes was determined using a sessile drop technique. The experiment was conducted on a Goniometer (Model: Kruss Gambult, Germany) consisting of a computer–controlled automatic liquid deposition system and deionized water was used in measurements. A small drop of 0.3 μL of water was dropped on the surface of the membrane using a syringe, and three strands of membrane fibers were randomly chosen for contact angle measurements.

Porosity and pore size measurements

Membrane porosity (ε) was measured by the dry-wet weight method. The membrane fibers (10 pieces × 5 cm) were equilibrated in water for 5 hours. The membrane fibers were weighed after the adsorption of water and after being dried on filter paper. The membrane porosity was calculated using eqn (1).

$$\varepsilon = \frac{M_1 - M_2}{V \times \delta_{\text{water}}} \times 100\% \tag{1}$$

where, M_1 and M_2 are the weights of the wet and dry membrane (gram), respectively. V is the volume of the HF membrane (cm^3) and δ_{water} is the density of pure water (g cm^{-3}). Then, the pore size can be calculated by Guerout–Elford–Ferry eqn (2).

$$r_{\text{m}} = \sqrt{\frac{(2.9 - 1.75\varepsilon) \times 8\eta\iota Q}{\varepsilon \times A \times \Delta P}} \tag{2}$$

where η is water viscosity at 25 °C (8.9×10^{-4} Pa s), ι is membrane thickness (m), Q is permeate water per unit time (m^3 s^{-1}), A is the effective area of membrane (m^2), and ΔP is operational pressure (Pascal). The pore diameter of the HF membrane was calculated by multiplying r_{m} by 2.

Membrane performance

Membrane transport properties. The pure water flux (PWF), protein (BSA) rejection, and solute removal were measured to evaluate the performance of the developed HF membrane. The

PWF, BSA rejection, and solute removal by the fabricated HF membrane were calculated using eqn (3)–(5), respectively. Their performances were tested by using the set-up experiments in Fig. 3. The volumes of permeate were recorded after a stable water flux value was obtained under 1 bar of pressure.

$$J_W \text{ and } J_S = \frac{V}{A \times t} \tag{3}$$

$$R(\%) = \left(1 - \frac{C_P}{C_f}\right) \times 100\% \tag{4}$$

where J_W is the flux of the solute (L m^{-2} h^{-1}); J_S is the flux of the solute (mg m^{-2} h^{-1}), V is the volume of the permeate (L), C_p is the concentration of permeate (mg L^{-1}), C_f is the concentration of feed (mg L^{-1}) A is the effective surface area (m^2), and t is the time of the flux measurement (h). Tap water was used for the water flux measurements. Both solutions at water flux and solute flux measurement were mixed with phosphate buffer saline (PBS) to adjust the solution to be the same as body fluids. The water flux was measured for 1, 2, 3, and 4 hours, which represents the dialysis time during the treatment. While the removal or clearance percentage of the urea and p-cresol was calculated using eqn (5). The concentration of BSA was measured using a UV-vis spectrophotometer (Hach, DR, 5000, Canada) under the wavelength 280 nm.

$$\text{Removal or clearance percentage } (\%) = \frac{C_0 - C_t}{C_0} \times 100\% \tag{5}$$

where C_0 and C_t are the concentrations of solute at the initial time and the specified time (mg L^{-1}). Cresol removal was calculated for total removal, diffusive removal, and adsorptive removal. The 50 mg L^{-1} of p-cresol solution (500 mL) was placed in the feed beaker and then diffused using the experimental setup.

The total removal of p-cresol was measured from the final concentration in the feed solution beaker. While the diffusive removal was calculated by the concentrations of the p-cresol found in the permeate beaker. Then, the adsorptive removal was calculated as the difference concentration between total removal and diffusive removal.
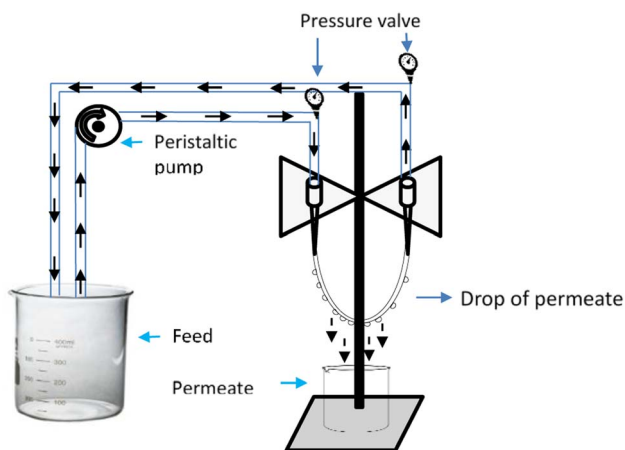

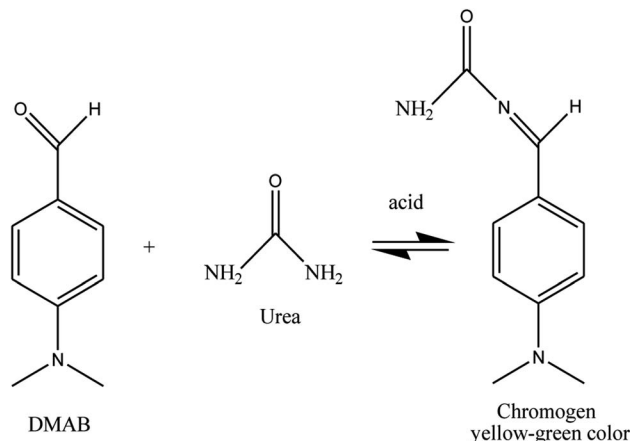Fig. 3 Schematic experimental set-up for cross-flow single hollow fiber membrane.

Fig. 4 Scheme of DMAB-urea reaction.

For the qualitative and quantitative analysis of urea, Ehrlich's reagent that contained p-dimethylaminobenzaldehyde (DMAB) was used. DMAB as a spectrophotometric reagent was coupled with ethyl alcohol and HCl to produce a complex agent. DMAB together with urea at ambient temperature produced a chromogen that shows a yellow-green color that can be detected using a UV-vis spectrophotometer (Fig. 4). The complex agent was prepared by dissolving 1.6 grams of DMAB in a small amount of ethyl alcohol, 10 mL of concentrated HCl was added subsequently and volume was made up to 100 mL using ethyl alcohol.[26] Then, 2 mL of urea was mixed with 2 mL of the complex agent, and the absorbance was measured at 420 nm using a UV-vis spectrophotometer. While p-cresol was measured at 282 nm directly without any treatment by using a UV-vis spectrophotometer.

Results and discussion

Previous research studies have demonstrated a more selective and more favorable for p-cresol removal, namely imprinted zeolite by p-cresol (IZC).[25] It was decided as a beneficial zeolite compared to zeolite non-imprinted commercial zeolite (ZeoY-C) and synthesized zeolite (ZeoY-S). IZC in powder form is very risky to be applied into hemoperfusion application for blood purification. It is due to the leaching effect of materials during the hemodialysis process. Therefore, in this research it was fabricated to become a hollow fiber mixed a matrix membrane (HF-MMM) incorporated with PES by the spinning process.

The effect of air gap distance

The air gap distance determines the time needed for the fiber to expose to the air during the spinning process. The air gap distance of the spinneret and coagulant bath played a crucial part in tailoring the hollow fiber membrane (HFM) in terms of outer and inner morphology as well as the size of the resulting lumen. These parameters are very important for the membrane separation performance.

In this study, the basic formulation of the dope solution was used PES/PVP (14/1.4). This is referred to Tijink et al. (2013)[27]

Table 2 The dope solution composition used in this study

Membrane	Percent composition (wt%)			
	PES	PVP	NMP	IZC
PES/PVP	14	1.4	84.6	—
PES/PVP/IZC	14	1.4	83.6	1

and Pavlenko *et al.* (2016)[17] who previously studied the application of the adsorbent incorporated into the polymeric membrane (MMM) applied in the HD treatment. The polymer loading used in this optimization was 14%. It was chosen caused the polymer then mixed with adsorbent, thus possible to increase the viscosity and impacted into the permeation.

Based on the experiment obtained, the viscosity of PES/PVP (14/1.4) was 2060.2 ± 0.21 cP and while it was incorporated with the adsorbent (PES/PVP/IZC (14/1.4/1)), it changed to 2305.8 ± 0.33 cP. In this optimization, the composition of the dope solution used is shown in Table 2. In this study, the neat

PES (PES/PVP) with PES incorporated with IZC as a filler (PES/PVP/IZC) were compared. The aim was to study the effect of IZC as a filler in terms of characterization and performance of the MMM developed.

The morphologies of the membrane for the outer surface and cross-sectional view studied by SEM for varied air gaps are shown in Fig. 5 and 6. The aim of the air gap study was to obtain better morphology of the membrane as well as the porosity, pore size, and separation performance for urea and *p*-cresol. Based on Fig. 5 and 6, the membranes produced have a porous structure on the outer surface as judged from the outer surface view and at the outer skin layer by the cross-sectional view. In the inner layer from the cross-sectional view, it showed that the produced membranes had a thin dense skin layer structure. This dense skin layer structure provides benefits to inhibit some compounds like albumin and red blood cells, which are still needed to cross the membrane. Additionally, the porous structure at the surface membranes helps uremic toxins pass
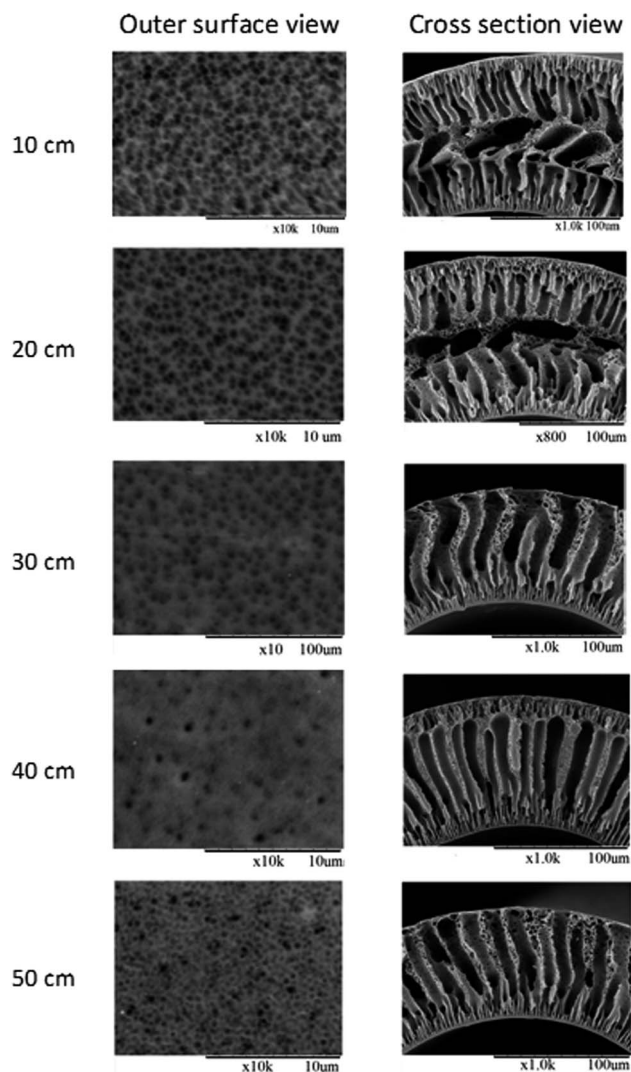

Fig. 5 SEM images for neat PES at varied air gaps.
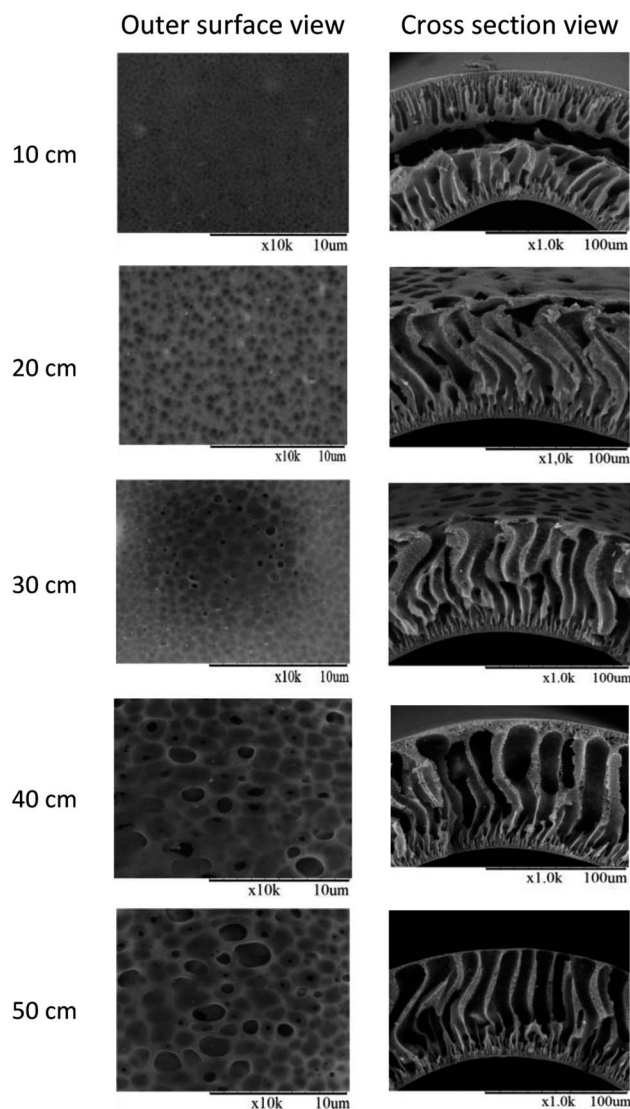

Fig. 6 SEM images for PES/PVP/IZC (14/1.4/1) at varied air gap.

through blood to the dialysate solution as a removal principle of dialysis. The obtained results show that there is no significant difference in the morphology between neat PES/PVP and when incorporated with IZC (PES/PVP/IZC).

The cross-sectional view for the air gap of less than 30 cm showed a sandwich-like structure, made up of two dense and finger-like structures. It is due to the solvent-moisture exchange at the outer surface of the membrane and was not caused by the very short residence time. In this situation, the bore fluid did not have more time to pass through from the inner side to the outer side before reaching the coagulant bath. Therefore, while the bore fluid reaches halfway to the outer side and solidified the inner side of the membrane, at the same time, the nascent hollow fiber reached the coagulant bath and solidified the outer side of the membrane. It succeeded to prompt precipitation on both sides and produced a sandwich-like structure. While the membranes spun at the air gap of more than 30 cm and produced a good finger-like structure from inner to the outer side. A little sponge-like materials at the membranes' outermost layer was formed due to the evaporation of the solvent (NMP) during dry spinning and a thin dense skin layer was formed at the innermost layer as a strong coagulant (water) was used.[28]

From the morphology, the sponge-like asymmetric structure was formed in the outermost layer at 40 cm of the air gap for both neat PES/PVP and PES/PVP/IZC. This sponge-like structure is highly favored, since it provides higher mechanical strengths and prevents membranes from leakages. It is perhaps happening in the finger-like macrovoid structure.[29] From the morphology studies, it is concluded that the air gap distance dramatically affects the morphology of the membrane produced.

The dimensions change for neat PES (PES/PVP) and PES/PVP/IZC at different air gap distances. The measurement of each membrane was measured in triplicate ($n = 3$). Based on the measurement, both the outer diameter (OD) and inner diameter (ID) sizes of the membrane were reduced by increasing the air gap distance.[30] The reducing value of OD and ID size is due to the elongation of the nascent fiber by gravity when it is passes through the air gap.[31] The OD/ID ratio for each air gap was similarly valued, it was around 1.9 for PES/PVP and 1.5 for PES/PVP/IZC. Reduced OD and ID sizes of membranes also reduced the membrane thickness. It promoted the greater removal of uremic toxins due to the distance to cross the membrane being shorter than the thicker membrane thickness.[32,33]

The air gap distance also affects the pore size, percentage porosity, and hydrophilicity, as can be seen from the WCA result of the membranes produced, as shown in Table 3. These parameters influenced the water permeation and BSA retention, which subsequently affected the uremic toxin removal during permeation. The higher air gap distance meant that nascent fiber was exposed for a longer time in the air and the gravitational effect caused the average pore size to be bigger than that at the lower air gap distance. The bigger pore size also increased the porosity.[34] Based on the experimental data obtained, the average pore size, porosity, and WCA for membranes produced are shown in Table 4. The results obtained with the increasing air gap indicated an increase in average pore size and porosity. It is due to the fact that shorter air gap distances eliminate the formation of microvoids. The membrane incorporated with IZC as a filler has a bigger pore size and porosity as the additional effect of the filler increased the viscosity of the dope solution. The average pore size obtained in this study was suitable to be applied to hemodialysis applications.

As shown in Table 3, the average pore size for PES/PVP was around 20 to 58 nm and PES/PVP/IZC was around 50 to 64 nm. It is quite small and good to be applied to hemodialysis. The bigger size could permit the loss of albumin and red blood cell during permeation. Based on the average pore size, hemodialysis membranes can be categorized as either nanofiltration or ultrafiltration. Ultrafiltration membrane has a pore size in the range of 10–100 nm, while nanofiltration membrane is in the range of 1–10 nm.[35] Additionally, it can be concluded that the

Table 3 Average pore size, porosity, and water contact angle for PES/PVP and PES/PVP/IZC at various air gap

	Average pore size (nm)		Porosity (%)		WCA (°)	
Air gap (cm)	PES/PVP (14/1.4)	PES/PVP/IZC (14/1.4/1)	PES/PVP (14/1.4)	PES/PVP/IZC (14/1.4/1)	PES/PVP (14/1.4)	PES/PVP/IZC (14/1.4/1)
10	23.83 ± 1.22	51.52 ± 1.13	31.75 ± 1.41	36.34 ± 1.20	89.52 ± 2.38	78.26 ± 3.98
20	33.82 ± 1.80	52.98 ± 1.18	32.16 ± 1.95	42.43 ± 1.04	85.07 ± 4.40	74.93 ± 5.15
30	45.68 ± 1.40	53.38 ± 0.70	40.12 ± 1.16	48.09 ± 1.06	82.97 ± 2.12	71.52 ± 3.20
40	49.28 ± 0.95	60.57 ± 1.25	43.65 ± 0.76	53.06 ± 1.15	81.23 ± 3.05	65.71 ± 2.16
50	58.38 ± 1.58	64.43 ± 0.98	45.65 ± 1.02	52.59 ± 1.49	76.77 ± 4.96	61.72 ± 2.03

Table 4 Dimensional of varying PES loading

PES loading (wt%)	Viscosity (cP)	Average pore size (nm)	OD (μm)	ID (μm)	OD/ID ratio	Dense skin layer (nm)
14	2305.8	60.56	450	288	1.56	268
16	2622.7	63.27	512	314	1.63	284
18	2991.2	71.36	576	347	1.66	443

membranes produced in this study can be categorized as ultrafiltration membranes.

The water contact angle (WCA) value is representative of the hydrophilicity of the membrane properties. Both the studied membranes have the same percentage of PES and PVP but different additional IZC as a filler. Based on the previous study,[25] of the IZC have a Si/Al ratio of 2.84. It indicates that IZC is a hydrophilic material. Furthermore, the IZC has a good impact on the hydrophilicity of the membrane while being incorporated into the membrane. Based on the calculation obtained, the impregnation of IZC into the membrane is able to improve the hydrophilicity of the membrane from 12 to 19%. It is a great effect on the produced membrane to be applied to hemodialysis. Hydrophilicity is one of the important features for water flux, BSA retention, and uremic toxins removal. The water contact angle was smaller with increasing air gap distance. It meant that the membranes were more hydrophilic.

Pure water permeability (PWP) or known as pure water flux (PWF) is defined as the volume of the water that passed through a membrane per unit of time, per unit of area, and per unit of pressure.[35] Water flux is very influenced by the hydrophilicity of the membrane. As described above, increasing the air gap distance and the effect of the additional IZ as a filler increased the hydrophilicity, similar to that reported by Salimi *et al.* (2016).[36] Furthermore, by increasing the air gap distance it showed a greater value for water flux. It is because the air gap of 50 cm has a longer and larger finger-like structures. This structure promoted the diffusion of water to pass through the membrane from the inner side to outer side. The PWF of PES/PVP/IZC was starting from 18.42 L m^{-2} h^{-1} bar^{-1} for an air gap of 10 cm to 50.84 L m^{-2} h^{-1} bar^{-1} for an air gap of 50 cm. These values were greater than those for the PES/PVP membrane. The PES/PVP membrane has PWF of 3.64 L m^{-2} h^{-1} bar^{-1} for the air gap of 10 cm and 25.28 L m^{-2} h^{-1} bar^{-1} for the air gap 50 cm.

The BSA rejection was also influenced by the membranes' hydrophilicity. An increase in hydrophilicity affected the higher BSA rejection value, meaning that the BSA was retained to cross through the pores of the membrane and flowed to the retentate. It is because the properties of BSA were as hydrophobic and the developed membranes w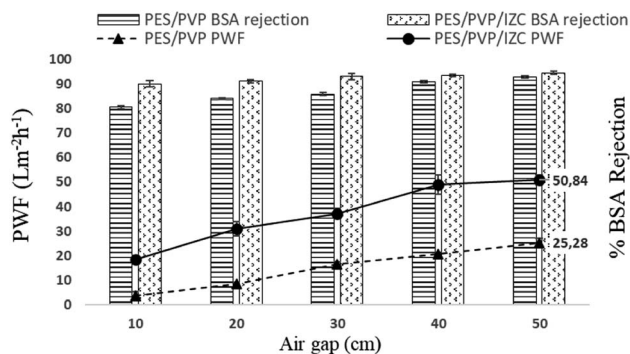ere hydrophilic. Based on Fig. 7, the membrane incorporated with IZC has a bigger BSA rejection compared to that without IZC as a filler, it is due to the IZC was an increase hydrophilicity membrane as mentioned before. This phenomenon also caused the formation of hydrophilicity on the membrane's surface, which could hinder protein to precipitate and consequently increase the rejection performance.[37] The longer air gap distance was increasing the percentage of BSA rejection of the membrane. The best BSA rejections for PES/PVP and PES/PVP/IZC were 92.88% and 94.59%, respectively. It was achieved by the longer air gap distance (50 cm). This achievement gave a good effect on the membrane properties. By increasing the BSA rejection, albumin blockage and albumin loss during permeation could be prevented.[38] Although the average pore size of the membrane at the longer air gap distance was bigger than the lower air gap, it did not significantly affect the BSA rejection. The experiment of Abidin *et al.* (2017) resulted that increasing the average pore size reduced the BSA rejection.[39] Hydrophilicity is the main factor influencing BSA rejection.

Fig. 8 and 9 depict the urea removal for PES/PVP (14/1.4) and PES/PVP/IZC (14/1.4/1), respectively, at varying air gaps starting from 10 to 50 cm. In view of the results obtained, the urea removal for every air gap was increased with the increasing air
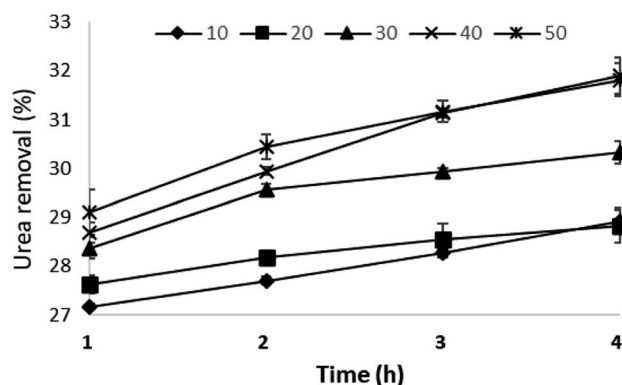

Fig. 8 Profile of urea removal for PES/PVP (14/1.4) at varying air gaps ($n = 3$).

Fig. 7 Profile of PWF and BSA rejection for PES/PVP and PES/PVP/IZC membrane for varying air gap ($n = 3$).
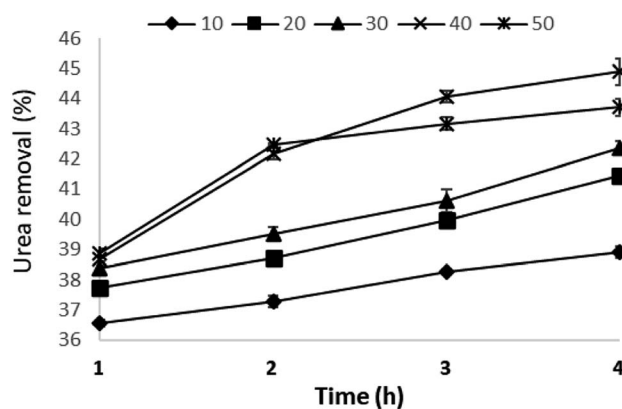

Fig. 9 Profile of urea removal for PES/PVP/IZC (14/1.4/1) at varying air gap ($n = 3$).

gap. As described previously, the increasing air gap affected the increasing average pore size, porosity, hydrophilicity, and PWF. Increasing these parameters automatically has an impact on increasing urea removal. It is because urea has a very small molecular size (60.056 g mol^{-1}) and belongs to the WSUT[40,41] Therefore, urea was very easily released through the pores of HF-MMM during filtration. Based on Fig. 8 and 9, show that PES blended by IZC has higher percentage removal for urea compared to neat PES. It caused the PES blended by IZC to have higher hydrophilicity compared to neat PES.

The same characteristic was also observed for the *p*-cresol removal using a PBS solution. As is known, *t p*-cresol has a small molecular size (108.14 g mol^{-1}) and is easily dissolved in water. Therefore, *p*-cresol removal increases with increasing the air gap. The results are shown in Fig. 10 and 11.

The maximum *p*-cresol removal achieved by neat PES was 21.55% at 3 hours of permeation for a 40 cm air gap distance. Then by incorporating IZC into the membrane, it was able to improve the *p*-cresol removal by up to 39.42% under the same conditions. The increasing *p*-cresol removal for PES blended by IZC was also affected by increasing the hydrophilicity. The 40 cm of air gap distance has better removal for urea and *p*-cresol because it has higher porosity (53.06%) compared to other air gap distances.

The total removal of *p*-cresol in PES incorporated by IZC is caused by diffusive and adsorptive removal in terms of diffusion and adsorption mechanism. It did not happen with the neat PES membrane. The diffusive removal was performed by *p*-cresol that permeated through the membrane pores. While the adsorptive removal was performed by *p*-cresol adsorbed or trapped by IZC insert in the membranes. By this mechanism, the developed membrane achieved the *p*-cresol removal of up to 34.49% by diffusion and 4.93% by adsorption. Additionally, it is worth mentioning that the adsorption capability of IZC blended into the membrane was extant. Therefore, considering the results obtained, the air gap distance of 40 cm was better than the others. According to the results obtained, it is proven that the addition of IZC can improve the membrane performance. Furthermore, the PES/PVP/IZC composition was better.

The effect of polymer loading

Polyethersulfone (PES) is one of the most common materials used to produce HD membranes besides cellulose triacetate, polysulfone, polyamide, polyacrylonitrile, and polymethyl methacrylate.[42] The fabrication of HF-MMM by using the dry/wet phase inversion spinning for each percentage of PES has been successfully fabricated. The morphology of the studied membranes is shown in Fig. 12. From the cross-sectional view, porous substructure and finger-like void structures from the inner to the outer edge are almost the same for varied polymer concentrations. Membranes studied contained micro-to macro-voids structures. The 14% PES loading had a larger finger-like macro-void structure, it is due to it having a lower polymer concentration then causing of non-solvent diffusion rate is faster than the solvent into polymer-poor phase.[43] The thicker dense skin layer on the innermost surface at 18% of PES loading is due to the demixing of the solvent and non-solvent during the phase inversion taking time compared to the lower polymer concentration, which can take place spontaneously. On the other hand, the thicker dense skin layer exhibited a higher polymer concentration. These phenomena were given a bad impact on the PWF and solute removal but neither on the BSA rejection. The dense structure helps in retaining albumin and red blood cells to cross through the membrane going outside, however, the thicker dense structure at the innermost layer is unfavorable for the removal of uremic toxins.

Additionally, from the outer and inner surface views, it can be observed that 16% of the PES loading has a better percentage porosity either in the inner and outer surfaces compared to 14
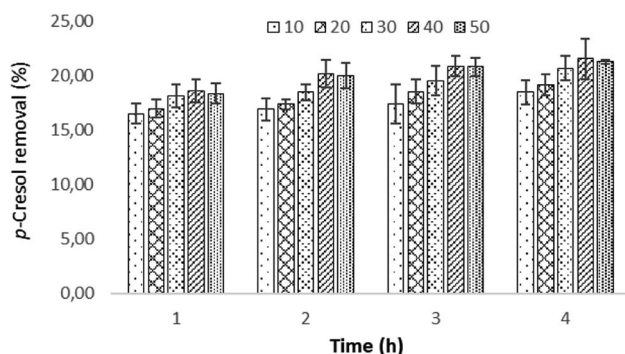
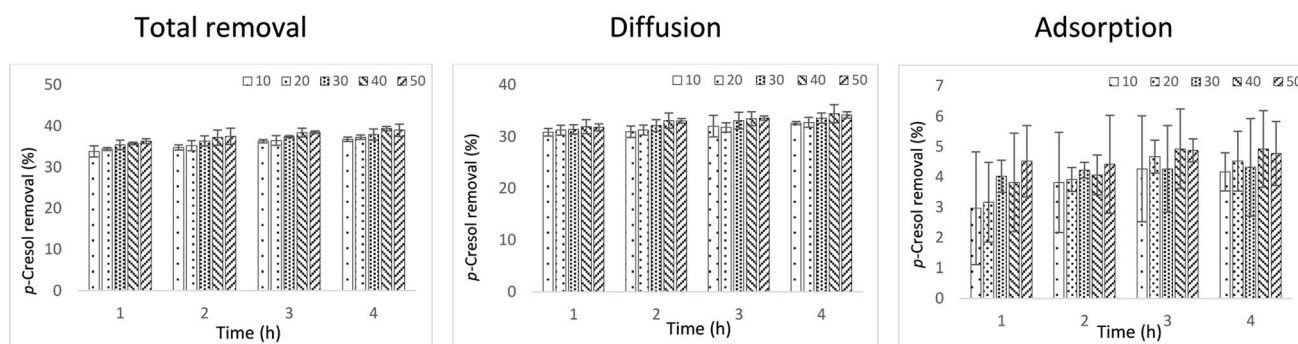**Fig. 10** Profile for *p*-cresol removal for PES/PVP (14/1.4) (*n* = 3).

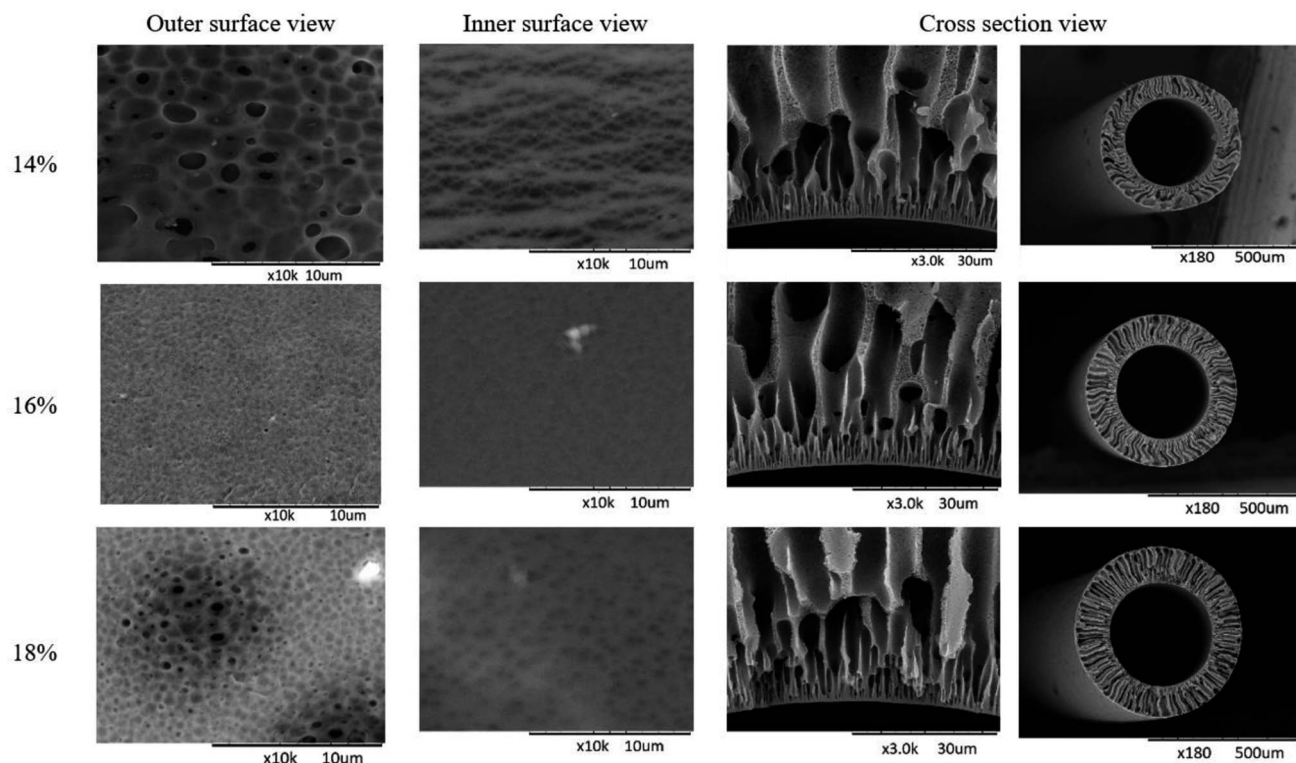**Fig. 11** Profile for *p*-cresol removal for PES/PVP/IZC (14/1.4/1) at varying air gap (*n* = 3).

Fig. 12 SEM images for fabricated membranes at varied PES loading and spun at 40 cm of air gap distance.

and 18% (Fig. 12). It is due to their differences in the viscosity. At 14% of PES loading, the average pores size was smaller compared to that in others. Although it is look like bigger than that in others for outer surface when viewed from the SEM images obtained at Fig. 12. It is because not every pores have a hole on the inside. While the 18% of PES loading also look bigger than the 16% of PES loading, the pores were not homogenous in size causing 18% of PES to be more viscous than 16%. Meanwhile, based on the obtained SEM images, 16% of PES loading have a small pores size and a better porosity compared to that with others loading.

Outer and inner diameter sizes of membranes can be seen in Table 4. The bigger size was achieved by 18% of PES loading. This phenomenon is because it has a bigger density compared to that observed with other loadings. The bigger OD/ID ratio shows the bigger wall thickness of the membrane. On the other hand, it was stated that the thicker wall membranes affect the diffusive removal rate of uremic toxins during filtration.[44] From the results obtained in the experiment, 18% of PES loading has a bigger wall thickness (229 μm) compared to 14% (162 μm) and 16% (198 μm) of PES loading. Further explanation will be described on this effect on the membrane characterization regarding hydrophilicity, water flux, BSA rejection, and performance in terms of urea and *p*-cresol removal obtained at each PES loading.

Excess water in the body is one symptom of kidney failure disease that has to be solved during the hemodialysis treatment.[45] It can have harmful effects of difficulty in breathing, high blood pressure, heart problems, discomfort, and swelling

or edema. By cleansing the water overload in the blood, the water–soluble uremic toxins are removed automatically at the same time. Therefore, water flux measurements are required to be tested during the development of HD membranes. Synthetic polymers, such as polysulfone (PSf) and PES, which are commonly used as the basic polymers in HD membranes are hydrophobic. To support the physical properties of PES, PVP was used as an additive to enhance hydrophilicity. Therefore, in this study, additional PVP loading was adjusted to the polymer loading (polymer/PVP ratio was 10). It is actually for knowing the real impact of the additional polymer loading on the membrane performance. The dope composition in this study was 14/1.4/1; 16/1.6/1; and 18/1.8/1 as described in Table 5.

The HF membranes produced in this study had lower water contact angles (65.71; 65.32; and 64.91 for 14, 16, and 18% PES loading, respectively) (Fig. 13). It indicates that the membranes studied were hydrophilic. From the obtained results, increasing the PES loading does not have a significant impact on the membrane's hydrophilicity. This is most likely due to the

Table 5 Dope composition for varying PES loading

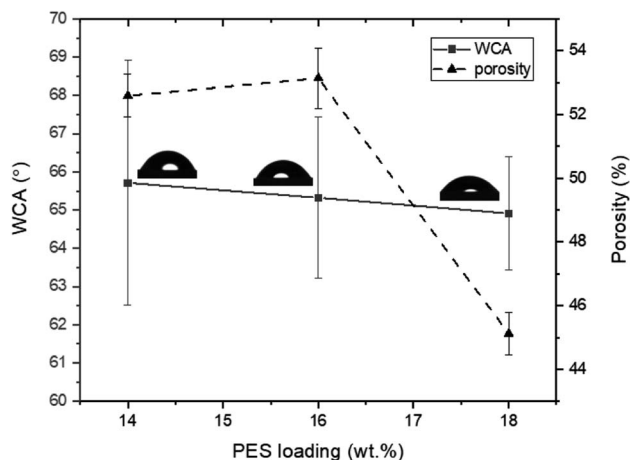| PES loading (wt%)	Percent composition (wt%)			
	PES	PVP	NMP	IZC
14	14	1.4	83.6	1
16	16	1.6	81.4	1
18	18	1.8	79.2	1

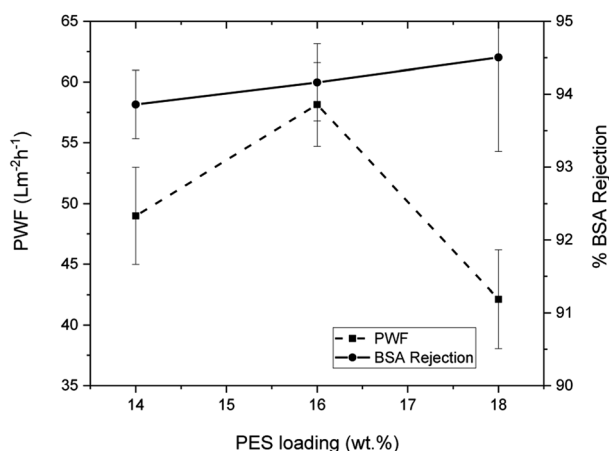Fig. 13 Profile of WCA and porosity at varying PES loadings of fabricated membranes, spun at 40 cm of air gap distance.

Fig. 14 Profile of PWF and BSA rejection at varying PES loadings of fabricated membranes, spun at 40 cm of air gap distance ($n = 3$).

Fig. 15 Profile of urea removal at varying PES loadings of fabricated membranes ($n = 3$).
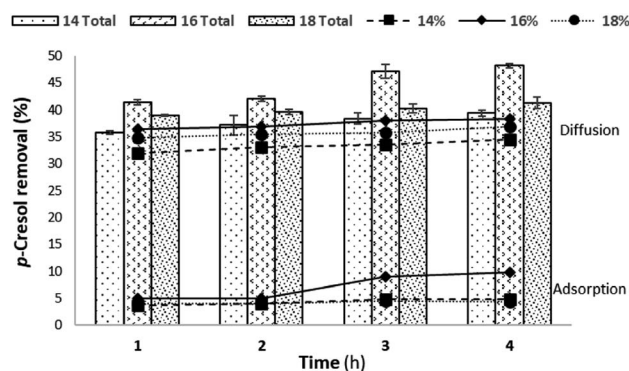
Fig. 16 Profile of p-cresol removal at varying PES loadings of fabricated membranes ($n = 3$).

influence of the PVP loading added. From the calculation, the increasing hydrophilicity of each increase in PES loading is the same value, which is equally 0.6%. These properties have a great impact on PWF and BSA rejection.

As shown in Fig. 14, the highest value of PWF was achieved by 16% PES loading, which is 58.15 L m^{-2} h^{-1}. It is because of its better porosity (53.14%) compared to that in other PES loadings (52.59% and 45.11% for 14% and 18% PES loadings, respectively). However, 16% of the PES loading has BSA rejection (94.16%) smaller than 18% for PES loading (94.50%) and higher than 14% for PES loading (93.66%). The best value of BSA rejection in this study was achieved at 18% of PES loading. It is due to the dense layer formed in the innermost surface was thicker than others, which restrained the BSA movement across the HF membrane.[32]

Fig. 15 shows that urea was removed up to 44.88, 48.46, and 44.48% by 14, 16, and 18% of PES loading, respectively, for 4 h of permeation. The best urea removal was achieved at 16%. This is because of a great PWF and percentage porosity compared to
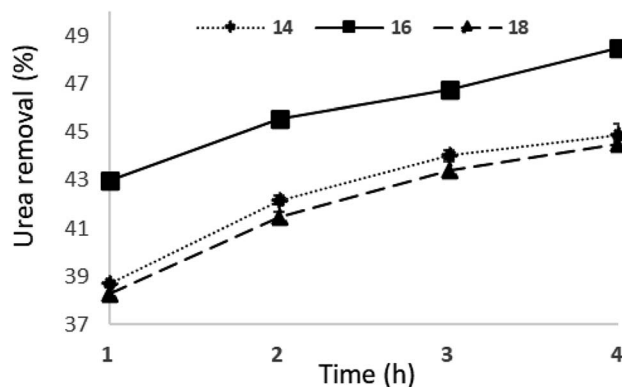
that of others. The great porosity also supported the removal of uremic toxins during the dialysis process.[46] In the studied membranes, urea removal gradually increased following the test permeation time starting from 1 to 4 h, as well as for p-cresol removal.

The best p-cresol removal was achieved at 16% PES loading (up to 48.14% in the 4 h permeation), as can be seen from Fig. 16. This phenomenon caused 16% to have a great PWF and percentage porosity. The 18% PES loading showed lower removal of urea and p-cresol because of it being thicker dense at the innermost layer compared to that in the other loadings.

Conclusions

The excellent developed HF-MMM was able to remove urea and p-cresol in one-step treatment. This membrane was able to carry out two mechanisms namely adsorption and diffusion without any constraints in terms of fouling and leaching of IZC, which is embedded into the membrane. The factor that affected the morphology and performance of the membrane was successfully investigated. It was found that 40 cm of the air gap distance and 16% of PES loading were chosen to get better morphology and performance. As a comparison with neat PES membrane, MMM was able to remove p-cresol 186.22 times higher. The

developed membrane was able to remove urea 60.74% and 66.29% for *p*-cresol using the BSA solution using the dialysis system with modules.

Conflicts of interest

The authors declare no conflicts of interest or personal relationships influencing the work in this study.

Acknowledgements

Notes and references

1 P. K. Samantaray, G. Madras and S. Bose, *Adv. Sustain. Syst.*, 2019, **3**(10), 1900017.

2 H. Zeng, S. He, S. S. Hosseini, B. Zhu and L. Shao, *Adv. Membr.*, 2022, **2**, 100015.

3 M. De Pascale, M. G. De Angelis and C. Boi, *Membranes*, 2022, **12**, 203.

4 W. L. Henrich, *Principles and Practice of Dialysis*, Lippincott Williams & Wilkins, USA, Fourth., 2009.

5 M. Ketteler, *Kidney Int*, 2006, **69**, 952–953.

6 M. Chelamcharla, J. K. Leypoldt and A. K. Cheung, *Semin. Nephrol.*, 2005, **25**, 81–89.

7 S. Yamamoto, J. J. Kazama, T. Wakamatsu, Y. Takahashi, Y. Kaneko, S. Goto and I. Narita, *Ren. Replace. Ther.*, 2016, **2**, 1–8.

8 K. Oshvandi, R. Kavyannejad, S. R. Borzuo and M. Gholyaf, *Nurs. Midwifery Stud.*, 2014, **3**(3), e21764.

9 J. Botella, P. M. Ghezzi and C. Sanz-Moreno, *Kidney Int. Suppl.*, 2000, **76**, S60–S65.

10 S. V. Mikhalovsky and V. G. Nikolaev, in *Activated Carbon Surfaces in Environmental Remediation*, ed. T. J. Bandosz, Elsevier Ltd, UK, 2006.

11 W. K. Cheah, K. Ishikawa, R. Othman and F. Y. Yeoh, *J. Biomed. Mater. Res., Part B*, 2017, **105**, 1232–1240.

12 C. Ronco, *Int. J. Artif. Organs*, 2006, **29**, 819–822.

13 M. S. L. Tijink, M. Wester, G. Glorieux, K. G. F. Gerritsen, J. Sun, P. C. Swart, Z. Borneman, M. Wessling, R. Vanholder, J. A. Joles and D. Stamatialis, *Biomaterials*, 2013, **34**, 7819–7828.

14 S.-Y. Suen, *J. Chem. Eng. Process Technol.*, 2015, **06**, 1–2.

15 M. Ulbricht, *Advanced Functional Polymer Membranes, Polymer*, 2006, **47**, 2217–2262.

16 M. Nidzhom, Z. Abidin, P. Sean, A. Fauzi, M. Ha, D. Othman, H. Hasbullah, N. Said, S. Hamimah, S. Abdul and F. Kamal, *Mater. Sci. Eng. C*, 2016, **68**, 540–550.

17 D. Pavlenko, E. van Geffen, M. J. van Steenbergen, G. Glorieux, R. Vanholder, K. G. F. Gerritsen and D. Stamatialis, *Sci. Rep.*, 2016, **6**, 34429.

18 J. Sun and L. Wu, *Colloids Surfaces B Biointerfaces*, 2014, **123**, 33–38.

19 S. B. Tantekin-Ersolmaz, C. Atalay-Oral, M. Tather, A. Erdem-Senatalar, B. Schoeman and J. Sterte, *J. Memb. Sci.*, 2000, **175**, 285–288.

20 M. Irfan and A. Idris, *Mater. Sci. Eng. C*, 2015, **56**, 574–592.

21 J. Cejka, A. Corma and S. Zones, *Zeolites and Catalysis: Synthesis, Reactions and Applications*, Wiley-VCH Verlag BmbH & Co. KGaA, vol. 1–2, 2010.

22 M. Zaarour, B. Dong, I. Naydenova, R. Retoux and S. Mintova, *Microporous Mesoporous Mater*, 2014, **189**, 11–21.

23 M. Khasanah, M. Harsini and A. A. Widati, *Indones. J. Chem.*, 2013, **13**, 108–113.

24 H. Chen, J. Wydra, X. Zhang, P. S. Lee, Z. Wang, W. Fan and M. Tsapatsis, *J. Am. Chem. Soc.*, 2011, **133**, 12390–12393.

25 Y. Raharjo, A. F. Ismail, M. H. D. Othman, N. A. N. N. Malek and D. Santoso, *Mater. Sci. Eng. C*, 2019, **103**, 109722.

26 C. P. Mahipalsinh, A. Agnihotri, A. I. Shaikh, S. I. Patel and K. D. Aparnathi, *Int. J. Chem. Stud.*, 2017, **5**, 1572–1576.

27 M. S. L. Tijink, M. Wester, J. Sun, A. Saris, L. A. M. Bolhuis-Versteeg, S. Saiful, J. A. Joles, Z. Borneman, M. Wessling and D. F. Stamatialis, *Acta Biomater.*, 2012, **8**, 2279–2287.

28 A. L. Ahmad, T. A. Otitoju and B. S. Ooi, *J. Ind. Eng. Chem.*, 2019, **70**, 35–50.

29 K. Sakai, *J. Chem. Eng. Jpn.*, 1997, **30**, 587–599.

30 R. X. Liu, X. Y. Qiao and T. S. Chung, *J. Memb. Sci.*, 2007, **294**, 103–114.

31 F. Korminouri, M. Rahbari-Sisakht, T. Matsuura and A. F. Ismail, *Chem. Eng. J.*, 2015, **264**, 453–461.

32 M. N. Z. Abidin, P. S. Goh, A. F. Ismail, M. H. D. Othman, H. Hasbullah, N. Said, S. H. S. A. Kadir, F. Kamal, M. S. Abdullah and B. C. Ng, *Mater. Sci. Eng. C*, 2017, **77**, 572–582.

33 M. N. Z. Abidin, P. S. Goh, A. F. Ismail, M. H. D. Othman, H. Hasbullah, N. Said, S. H. S. A. Kadir, F. Kamal, M. S. Abdullah and B. C. Ng, *Chem. Eng. Trans.*, 2017, **56**, 1609–1614.

34 N. Peng, T. S. Chung and K. Y. Wang, *J. Memb. Sci.*, 2008, **318**, 363–372.

35 M. Mulder, *Basic Principles of Membrane Technology*, Kluwer Academic Publishers, Dordrecht, The Netherlands, 2nd edn, 1996.

36 E. Salimi, A. Ghaee, A. F. Ismail, M. Hafi and G. P. Sean, *Macromol. Mater. Eng.*, 2016, **301**, 771–800.

37 E. Salimi, A. Ghaee and A. F. Ismail, *RSC Adv*, 2016, **6**, 44480–44488.

38 Y. Raharjo, M. Z. Fahmi, S. Wafiroh, A. A. Widati, E. R. Amanda, A. F. Ismail, M. H. D. Othman and D. Santoso, *J. Teknol.*, 2019, **81**, 137–144.

39 N. Said, H. Hasbullah, A. F. Ismail, M. H. D. Othman, P. S. Goh, M. N. Zainol Abidin, S. H. Sheikh Abdul Kadir, F. Kamal, M. S. Abdullah and B. C. Ng, *Polym. Int.*, 2017, **66**(11), 1424–1429.

40 M. Wester, F. Simonis, N. Lachkar, W. K. Wodzig, F. J. Meuwissen, J. P. Kooman, W. H. Boer, J. A. Joles and K. G. Gerritsen, *Artif. Organs*, 2014, **38**(12), 998–1006.

41 M. S. L. Tijink, J. Kooman, M. Wester, J. Sun, S. Saiful, J. A. Joles, Z. Borneman, M. Wessling and D. F. Stamatialis, *Blood Purif*, 2014, **37**, 1–3.

42 K. Sakai and M. Matsuda, in *High-Performance Membrane Dialyzers*, ed. A. Saito, H. Kawanishi, A. C. Yamashita and M. Mineshima, Karger, Basel, 2011, vol. 173, pp. 11–22.

43 N. M. Ismail, N. R. Jakariah, N. Bolong, S. M. Anissuzaman, N. A. H. M. Nordin and A. R. Razali, *J. Appl. Membr. Sci. Technol.*, 2017, **21**, 33–41.

44 C. Ronco and W. R. Clark, *Nat. Rev. Nephrol.*, 2018, **14**, 394–410.

45 N. Said, H. Hasbullah, A. Fauzi and M. Nidzhom, *Chem. Eng. Trans.*, 2017, **56**, 1591–1596.

46 N. J. Kaleekkal, A. Thanigaivelan, M. Tarun and D. Mohan, *Chinese J. Chem. Eng.*, 2015, **23**, 1236–1244.